

---

## Microstructure and tensile properties of carbon-epoxy laminates produced by automated fibre placement: Influence of a caul plate on the effects of gap and overlap embedded defects

Lan Marine <sup>1,\*</sup>, Cartié Denis <sup>2</sup>, Davies Peter <sup>3</sup>, Baley Christophe <sup>1</sup>

<sup>1</sup> University of South Brittany, LIMATB, Rue de Saint Maudé, 56000 Lorient, France

<sup>2</sup> Coriolis Composites SAS, Rue Condorcet, Z.A. du Mourillon, 56350 Quéven, France

<sup>3</sup> Ifremer, Centre Bretagne, Technopôle Brest Iroise, 29280 Plouzané, France

\* Corresponding author : Marine Lan, email address : [marine.lan@univ-ubs.fr](mailto:marine.lan@univ-ubs.fr)

---

### Abstract :

Automated fibre placement (AFP) enables the trajectory of unidirectional composite tape to be optimized, but laying down complex shapes with this technology can result in the introduction of defects. The aim of this experimental study is to investigate the influence of gaps and overlaps on the microstructure and tensile properties of carbon-epoxy laminates. First, a comparison between a hand-layup and AFP layup, draped and cured under the same conditions, shows equivalent microstructures and tensile properties. This provides the reference values for the study. Then, gap and overlap embedded defects (more or less severe) are introduced during manufacturing, on two cross-ply layups [(0°/(90°)5/0°)] and [(90°/0°)2/90°]. Autoclave cure without a caul plate results in local thickness variation and microstructural changes which depend on the defect type. This has a strong influence on mechanical performance. Use of a caul plate avoids these variations and in this case embedded defects hardly affect tensile properties.

**Keywords :** A. Carbon fibres, B. Automated layup, C. Defects, D. Mechanical properties

## 1. INTRODUCTION

Composite materials have been used for many years in the aeronautical industry to reduce aircraft weight and to optimize performance. The traditional manufacturing techniques are being required to produce increasingly complex shapes while reducing defect levels. In order to address this, new processes such as AFP (Automated Fibre Placement) have been developed, which allow the optimization of reinforcement lay-up and close control of process parameters [1]. An automated fibre placement machine applies tows (of 3.175 mm to 12.7 mm width), in the form of a ribbon of unidirectional prepreg with fibres in either thermosetting or thermoplastic matrix but also powder tows for RTM, onto the surface of a mould through a placement head. Thirty-two tows may be placed simultaneously side by side on the mould surface. The orientation of plies, the precision of draping, repeatability and reliability of manufactured parts is ensured while reducing mechanical tolerances. This technology has the advantage of making parts of complex curvilinear shapes, with single or double curvature, in order to optimize the composite structure [2]. It is also possible to produce laminates with large thickness variations. The combinations of controlled pressure exerted by roller compaction and the local application of temperature by a heating system (infrared lamp or hot air torches) removes air trapped between the layers, reduces porosity and allows the adhesion of different plies of the laminate to the mould or onto previously draped plies [3–5]. Following the layup, the manufactured part is placed in an autoclave to consolidate the laminate plies, polymerizing the resin contained in the prepreg tapes. Mechanical tests on specimens from laminated AFP components have highlighted an increase in buckling load [6,7], reduced effects of stress concentrations [8,9] and reduced notch sensitivity [10].

During the layup of composite parts by AFP, gaps and overlaps are generally avoided so as not to impact on the mechanical properties. However, aircraft manufacturers impose a gap of

0.5 mm between each series of  $n$  ribbons, with  $n$  depending on the placement head used for draping. Figure 1 illustrates this rule for a tape laying head of  $n = 8$  ribbons. This gap prevents the creation of an overlap which is generally forbidden by the aircraft manufacturers. The value of this gap is defined according to the machine tolerances.

During the draping of non-developable surfaces, misalignment of the tows' edges will be induced, so management of the gap and/or overlap will be necessary. The AFP programming software allows optimization of the positioning of the tow drop offs. This option allows the location of singularities and their dimensions to be understood, but discontinuities may occur. The tows are cut perpendicular to the fibres and this may create heterogeneous areas depending on the draping strategy. In addition, gaps and tape overlaps, directly related to machine and material tolerances, can be introduced and affect the mechanical properties of the manufactured parts. Research has been conducted for many years to understand the impact of these constraints on carbon fibre reinforced thermoset materials. There are now methods which allow the tape laying trajectory to be optimized, to reduce the impact on mechanical properties [11–13].

Sawicki et al. [14] modelled the influence of gaps and overlaps in plies oriented at  $90^\circ$  to the loading direction in compression. Ply waviness in defect regions resulted in a loss of compression strength. Blom et al. [15] presented a numerical investigation of the compression behaviour that showed the effect of the tow drop areas on AFP laminate panel properties. They concluded that a significant decrease of the strength and the stiffness results when the numbers of tows per course increases. The position of the tow drop area influences the strength and the stress distribution. Turoski [16] performed experimental and numerical tests to investigate the impact of the number of gaps (one, two, three or four) and offset of gap on the tensile and compression strength for unnotched and notched quasi-isotropic laminates. He showed that in tension, the gaps have a smaller effect than when there is an open hole. For

compression, unnotched and notched samples showed failure stress reductions as the number of gaps increases. In general, the compression tests revealed larger variations than the tension tests. These previous studies show that the losses in mechanical properties are mainly due to modifications to the geometry in the gap area, related to thickness variation and out-of-plane ply waviness.

Croft et al. [17] presented results from an experimental study which allowed the influence of the main defects (gap, overlap, half spacing /overlap defects and twisting) to be quantified for laminates loaded in tension, compression and shear. They showed that defects present along the specimen length caused a larger drop in mechanical properties than defects across the specimen width. Open-hole test specimens showed a larger variation in properties due to fibre waviness near defects, which initiated micro-buckling. For open hole compression [18], gaps and overlaps have a limited effect when they are placed in the loading direction. When plies are oriented at  $90^\circ$ , the fibre waviness causes a drop in properties. More recently, Falco et al. [19] studied the effect of fibre angle discontinuities on the un-notched and open-hole tensile strength of quasi-isotropic laminates. Observation of the geometry of embedded defects and the resulting mechanical behaviour showed that the influence of gaps was more significant when staggering rules (offsetting of the defects in successive plies) were not applied. However the test results showed that an open hole has a stronger negative influence than that of a gap singularity. The effects of impact and compression after impact were also studied, experimentally and numerically [20,21].

Li et al. [22] developed a 3D meshing tool to automatically generate gaps and overlaps numerically. This enabled them to investigate the thickness variations associated with singularities, as well as out-of-plane ply waviness. Models with different sizes and distributions of gaps and overlaps were set up in order to study how these singularities affect properties. Numerical studies have also been performed to examine the influence of gap and

overlap defects on the in-plane stiffness and buckling of laminates laid up by AFP [23–25]. These indicate that overlaps can result in an increase in properties, in contrast to gaps which tend to weaken these materials.

The aim of the work presented here is to develop an experimental method for the analysis of the consequences of the presence of singularities, which are introduced by AFP, for the mechanical properties of carbon/epoxy laminates. Two singularity configurations, gaps and overlaps, of different geometries, have been deliberately introduced into laminates with different stacking sequences, in order to examine how they affect tensile properties. The sequences are only based on  $0^\circ$  and  $90^\circ$  layers and are loaded in tension to avoid membrane-bending coupling. First, a comparison is made between a plate produced by hand layup and one made by AFP, without embedded defects, in order to provide reference values. Then plates with two stacking sequences but the same number of  $0^\circ$  plies,  $[0^\circ/90^\circ_5/0^\circ]$  and  $[(90^\circ/0^\circ)_2/90^\circ]$ , were prepared with embedded defects. These sequences were chosen to study first an extreme case, with superposed embedded defects, then a more realistic case. The embedded defects were only introduced in the  $90^\circ$  plies. C-scan inspections were used to check the quality of all plates. Then scanning electron microscopy (SEM) was used to examine the microstructure of the stacks at the location of embedded defects in detail. Finally, tensile loading enabled the influence of the embedded defects on tensile properties to be quantified. Plates were cured both with and without a caul plate; caul plates are often but not always used during cure in the aeronautical industry. The influence of this plate is examined as it has a strong effect on both geometry and microstructure, but few systematic studies of caul plate effects on AFP composite performance are available.

## 2. MATERIALS AND METHODS

### 2.1. Material

The material studied is carbon-reinforced prepreg (8552/AS4/RC34/AW194) from Hexcel Composites [26]. The nominal baseline fibre volume fraction and the nominal cured ply thickness are respectively  $57 \pm 2 \%$  and  $0.18 \pm 0.01$  mm. Three samples were taken from different areas in each panel and analyzed to obtain these values. In the case of manual layup, the prepreg is used directly in its original configuration as unidirectional bands. In the case of draping with the fibre placement process, the prepreg is presented as a tow of width  $6.35 \pm 0.25$  mm. The unidirectional bands and the tows come from the same batch of material in order to compare the properties.

### 2.2. Manufacture of samples

To manufacture the different plates (400 mm wide by 500 mm long), the robotic arm and placement head developed by Coriolis Composite were used [27]. This enabled 8 prepreg fibre tows to be draped simultaneously with a total width of 50.8 mm ( $8 \times 6.35$  mm) per course. Heating was by an IR lamp which provides localized heat to enhance adhesion between the successive plies. A compaction force of 100 N was applied during the draping operation. The draping speed was 0.1 m/s. To obtain a smooth surface, the first ply was draped over a film of Teflon Wrightlon 5200 supplied by Airtech® maintained by vacuum. Finally, to make a gap or overlap, the software of the fibre placement machine was programmed by indicating in the draping program either not to place a tow or to place an extra tow.

### 2.3. Processing cycle

The autoclave cycle imposed on samples respects the conditions of polymerization of pre-impregnated carbon/epoxy provided by the supplier of the material (110°C during 60 min followed by 180°C for 120 min with a maximum autoclave pressure of 7 bars).

The specifications of aircraft manufacturers for the autoclave polymerization of structural parts sometimes require the application of a caul plate acting as a backing mould. This caul plate is generally made of thin metal or CFRP laminate, positioned within the vacuum bag. The purpose of this caul plate is to allow a better final consolidation of parts and a smooth surface finish. To determine the influence of this caul plate on the microstructure of lay-ups draped by AFP, a series of plates containing defects was polymerized without a caul plate. All the other plates of this study were polymerized according to the specifications of aircraft manufacturers with a 2 mm thick aluminium caul plate. Wriathlon 5200 release film supplied by Airtech® were used between to mould surface and the panel as well as between the panel and the caul plate to permit the flow of the material.

### 2.4. Ultrasonic C-Scan inspections

For this study, ultrasonic C-Scan was chosen for analysis of the sample material health. The ultrasonic C-scan equipment (Sofratest 49944) used for the inspections was equipped with a transducer and a plane aluminium panel acting as a reflector. For these inspections, the plates were placed on the reflector on spacers and immersed in a tank containing water. The control was performed by a focused transducer, with a frequency of 10 MHz and a focalization length of 76 mm, which scans in the X and Y directions thanks to a motorized system that allows the entire surface of the part to be covered. The acquisition step is one millimeter, in all cases a measurement was made at the centre of the defect region .

## 2.5. SEM analysis

The morphology of embedded defects and the organization of plies have been observed with a Jeol JSM 6460 LV scanning electron microscope (SEM). The area examined was located in the middle of the plates, where the defects introduced during the layup were located. The samples were cut then polished to 1 micron in order to obtain flat, clean surfaces before examination.

## 2.6. Image analysis

Fibre volume fraction and porosity levels were determined using image analysis of SEM images with *ImageJ* software. Assemblies of several images were necessary to re-create all the zones affected by the embedded defects. Contrast was first adjusted, to reveal fibres, matrix and porosity. The software then quantified the amount of each.

## 2.7. Mechanical experiments

Standard tensile tests were carried out according to the ASTM D3039 [28]. In order to measure the influence of defects on the mechanical properties in the most critical situation, defects were placed in the middle of the sample, perpendicular to the direction of tensile loading (Figure 2). These tests were performed on an Instron hydraulic test machine, with a load cell of 50 kN, at a loading rate of 2 mm/min. In order to limit stress concentrations that may be caused by the clamping system of the tensile testing machine and to avoid premature failure, aluminium tabs of 2 mm thickness were bonded to each end of the specimen using a two component epoxy adhesive. For each configuration, an average of eight specimens was tested.

The Aramis® (GOM, Germany) optical system was used in these tests to measure the full-field displacements and strains on the outer plies with Digital Image Correlation. Longitudinal

strain gauges were also positioned on the other side of the specimen in three locations (one at the middle of specimen and one at each end) to check strain values.

### 3. RESULTS AND DISCUSSION

#### 3.1. Comparative study of hand layup and layup by AFP

Two plates consisting of 7 plies with a  $[(0^\circ/90^\circ)_3/0^\circ]$  stacking sequence were laid up. The first was laid by hand, using standard industrial practice. The second was laid up by AFP with bands cut from the same roll of prepreg as the hand lay-up plate, applying an aeronautical procedure (respecting a space of 0.5mm between each passage of the placement head, Figure 1). The two plates were cured at the same time in the same autoclave with caul plates.

C-Scan and SEM observations revealed the microstructure of both composites. Fibre volume fractions were determined to be 58.5 % and 59.7 % for the hand and AFP lay-ups respectively. Impregnation quality was good for both, see Figure 3 (i) and Figure 3 (ii), with low porosity levels around 0.01% and 0.02%. Only a small number of micro porosities, of diameters similar to carbon fibre diameter, were noted in interply regions.

The final thickness of both materials was similar as will be shown below. Tensile tests on the two materials showed very similar properties, with modulus values close to the estimated value of 84.8 GPa based on suppliers' fibre and matrix properties (the theoretical longitudinal modulus and the theoretical transverse modulus are respectively 141 GPa and 10 GPa).

There is no significant difference between the microstructures or the tensile properties for plates layup by hand or AFP then cured with a caul plate, so these values will now be used as a reference to examine the influence of embedded defects .

### 3.2. Stacking with embedded defects in five superimposed plies

The aim of the first series of tests was to introduce extreme examples of superposed gaps and overlaps into a sensitive stacking sequence in order to assess their effects. It should be emphasized that this is a very severe test case.

Two series of four plates, each with seven plies  $[0^\circ/90^\circ_5/0^\circ]$ , were manufactured by AFP. A reference plate was produced with the same sequence at the same time for comparison. The defects have been designed to represent the most critical situations. Indeed, they were introduced into the plies oriented at  $90^\circ$  and superimposed on each other at the centre of each of the plates, Figure 4. The dimensions of the defects have also been exaggerated to accentuate their effects on mechanical properties. They are equivalent to either half the width of a tow (3.175 mm) or the complete width (6.35 mm).

The first configuration plate studied is draped manually from unidirectional plies, Figure 4 (i). This plate is the reference plate which contains no singularity. The second configuration studied is a gap of 0.5 mm, Figure 4 (ii), imposed between each passage of the placement head. This plate is considered to be the aeronautical reference for the AFP process. The third configuration, Figure 4 (iii) studied is a gap of 3.175 mm. This singularity is obtained by programming a gap of the equivalent of half tow in the center of the plate in each  $90^\circ$  plies. This defect is commonly induced during the production of curved parts when passing from one sector to another. The fourth pattern corresponds to the creation of a gap of 6.35 mm width, Figure 4 (iv). This configuration simulates the absence of a ribbon in the centre of the plate in  $90^\circ$  oriented plies. The last configuration studied corresponds to an overlap of 3.175 mm, Figure 4 (v). This configuration corresponds to addition of the equivalent of a half-tow at the centre of the plate and thus creates a local extra thickness of the plies at  $90^\circ$ . This defect may arise during the manufacture of a complex shape which results in a variation of the position of the ribbons.

The first series of four plates was manufactured with a caul plate. A second series of four plates with exactly the same stacking sequence and embedded defects was then produced without the caul plate. C-scan inspection of all plates indicated no significant defects outside the singularity regions. Only a variation in thickness revealed the presence of defects in samples cured without a caul plate.

Observation of the material microstructure is essential in order to understand the influence of gap and overlap defects, so all plates were examined. SEM micrographs of the hand layup and AFP reference plates are shown in Figure 5 (i) and Figure 5 (ii) and reveal good quality laminates and similar thicknesses. Plates with gap defects (3.175 mm and 6.35 mm) reveal a quite different microstructure depending on whether a caul plate is used or not, Figure 5 (iii) and Figure 5 (iv). The large white regions in these images are unreinforced resin. When no caul plate is used there is a local significant reduction in plate thickness. For the 6.35mm gap the 5 plies at  $90^\circ$  are no longer visible in the gap area. The use of a caul plate for plates with the same allows the gaps to be filled during cure and only the appearance of resin rich regions at the  $0^\circ/90^\circ$  interface reveals their presence. For the overlap a local increase in thickness is noted (Figure 5 (v)), which is reduced by the presence of the caul plate.

The pressure exerted by the caul plate assists the movement of the material in the singularity zone during autoclave cure and compacting is more homogeneous, limiting porosity development near the embedded defects. The cure step is critical in determining the final microstructure and the caul plate limits the thickness variations in the length of samples, introduced during lay-up, as shown in Figure 6. These values were determined with a micrometer and checked by image analysis of SEM images. Values for the distance over which there is a variation in microstructure, i.e. the zone where ply waviness or swelling of the  $0^\circ$  plies occurs due to the presence of the embedded defects, vary considerably. If caul

plates are not used large thickness variations are noted except for the reference plates (0.5mm gap).

Figure 7 shows an example of stress-strain plots for 6.35mm gap specimens with and without caul plates. Two plots of apparent stress are shown for the case without caul plate, one using the local thickness at the gap and a second using the thickness away from the gap; it is clear that locally the stress is much higher, but in the gap region only  $0^\circ$  plies are present, elsewhere in the specimen the response is similar to that of the plates with caul plates. Figure 8 shows examples of strain measurements.

The modulus values from all the tests are shown in Figure 9. These are calculated using the local thickness to determine the stress, and strain measurements in the embedded defect region, the latter obtained using DIC. It should be emphasized that these are apparent modulus values strongly influenced by both the  $0^\circ$  plies remaining when  $90^\circ$  reinforcement leaves the zone and by the modified thickness. The theoretical modulus of this laminates is 47.4 GPa. There is no significant variation for specimens with embedded defects, values vary by about 4% compared to the AFP reference value in zones away from the singularity. The absence of a caul plate does not affect this value either. In the specimen centre close to the singularity, the absence of a caul plate results in significant thickness and microstructure variations as shown above, and this is reflected in the local moduli. When the caul plate is employed the differences are small, a maximum variation of 14% is measured. Gap defects reduce thickness and increase local modulus while overlaps increase thickness and reduce modulus.

Sample strength can be evaluated in terms of load flux, a tensile load normalized by specimen width but not including thickness. These values are shown in Figure 10. For the specimens manufactured with a caul plate these values vary little when embedded defects are introduced. For plates cured without caul plates however, the presence of gaps and embedded defects result in significant drops in load flux, with a reduction of 35% for the overlaps.

The failure behaviour can also be analysed using an apparent stress estimated for the central zone of the sample using the measured local thickness, Figure 11. These tests are performed with the loading in the direction perpendicular to the 5 plies at 90°, but final failure is governed by the two outer plies at 0°. For specimens from the plate cured with a caul plate final failures are randomly distributed along the specimens when embedded defects are present. The small variations in stress correspond to the very small thickness variations. When caul plates were not employed all failures occurred at the embedded defects except for the reference AFP specimens. The large variation in apparent strengths for the latter is a result of both thickness variations and local ply orientation. The gap of 6.35 mm leads to swelling of the 0° plies due to the significant presence of excess resin. The absence of 90° fibres leads to an increase of the apparent strength, while the 3.175 mm overlap causes a local increase in thickness and a drop in local 90° fibre content resulting in a large drop in break stress.

In summary, the use of a caul plate ensures that the applied autoclave pressure is mostly reacted at high thickness spots in the lay-up, generating the localised pressure gradients that are needed to cause flow to equalize the thickness. As a result the influence of gap and overlap defects on tensile properties are very small even for this extreme [0°/90°<sub>5</sub>/0°] stacking sequence with superposed embedded defects. Without the caul plate during cure the large thickness and microstructure variations can promote either higher or lower properties.

The stacking sequence adopted in this first study, with singularities superposed in the centre of the plate, is an extreme situation. The lay-up rules applied in the aeronautical industry are designed to avoid such a “worst case”, and the fibre placement robots are equipped to detect missing tapes during lay-up. In order to complete this study of the influence of caul plates on embedded defects a second more traditional lay-up was therefore examined.

### 3.3. Stacking with embedded defects in single ply

The aim of this second part of the study was to examine the influence of gap and overlap defects on an alternating ply laminate. This stacking sequence,  $[(90^\circ/0^\circ)_2/90^\circ]$ , is manufactured in a more standard fashion by alternating the  $0^\circ$  and  $90^\circ$  plies and would be expected to be more sensitive to defects as the single alternating plies will restrict flow during cure to a greater extent than in the previous laminate, which contained a block of similar plies. Two series, each of four plates, were manufactured by AFP, with the same embedded defects as in the first part of the study, with and without caul plates, Figure 12. A hand lay-up reference plate was also made. The embedded defects were introduced into the central ply at  $90^\circ$ . The other plies respected the 0.5 mm gap between passes, as shown in Figure 1.

All plates were inspected by C-scan and no macro-porosities were revealed. Only a thickness variation was noted near the gaps and overlap for the plates cured without caul plates. For the plates with 0.5 mm gaps there was no influence of the caul plate on the microstructure. For the plates with gap of 3.175 and 6.35 mm ( Figure 13), the microstructures are similar, with resin-rich zones and missing  $90^\circ$  reinforcement in the central ply. The caul plate again results in significantly reduced thickness variations for all the alternate ply laminates compared to those without caul plates, Figure 14. However, the singularity is not completely filled even with the caul plate due to the restricting effect of adjacent plies on material movement (Figure 3 (ii) ). When an overlap is introduced in the central ply, there is an over-thickness with and without the caul plate, but the microstructure is less disturbed when the caul plate is present.

Figure 15 shows the measured moduli values. The theoretical modulus of this laminates is 62.4 GPa. The variations in this modulus for specimens with defects, at the specimen ends, are not significant even for cure without a caul plate (less than 6%). In the central sections close to the embedded defects, a small drop is noted for specimens with caul plates, due to

the small variation in microstructure. When there is no caul plate a marked influence of the singularity is apparent as a result of reduced local thickness (Figure 14).

Figure 16 shows the load flux at failure and it is interesting to note that there is no significant influence of these embedded defects, with or without caul plate. The variations in thickness do not affect the ability of the material to transfer load as the  $0^\circ$  plies are in place and there is no global stress concentration effect in the singularity region.

Figure 17 shows the local apparent stresses at failure estimated in the singularity region. Again, as for the previous stacking sequence when caul plates are used the failures occur randomly along the specimens. A maximum variation of tensile properties of 5% is measured between the AFP reference plate and the plate containing an overlap. Without caul plates the failures occur close to the singularity and here the apparent break stresses tend to increase as thickness decreases, but even for the overlap case there is no drop in stress compared to the reference values.

In summary for this alternate ply stacking sequence the caul plate is less effective in homogenizing the material at gaps and overlaps than for the sequence with a block of  $90^\circ$  plies. However, in spite of significant thickness variations, particularly if caul plates are not used during cure, the properties in tension vary very little in spite of large initial embedded defects.

#### 4. CONCLUSION

In the present experimental study, the influence of the presence of a caul plate during cure has been quantified for different gap and overlap defects. Both microstructure and tensile behaviour of two cross-ply layups  $[0^\circ/90^\circ_5/0^\circ]$  and  $[(90^\circ/0^\circ)_2/90^\circ]$  have been examined.

A first comparison between specimens draped manually and draped by AFP indicated no differences between either the microstructure of the laminates or their mechanical properties, and provided baseline reference values.

Different gap and overlap singularities were then introduced. First, an extremely severe stacking sequence was studied,  $[0^\circ/90^\circ_5/0^\circ]$  with five superposed embedded defects. The presence of a caul plate during cure reduces thickness variations and encourages resin flow so that even large singularities are attenuated, and tensile properties vary by less than 10% with respect to the reference values. Without the caul plate large thickness variations and resin-rich regions cause significant changes in tensile properties.

In a second series of tests a more realistic stacking sequence was employed,  $[(90^\circ/0^\circ)_2/90^\circ]$ , with embedded defects in only one ply. In this case the defects remain after cure but their dimensions are reduced. Again, tensile properties change little with a caul plate but the absence of a caul plate results in property changes due to local thickness variations.

Overall, in spite of the introduction of large embedded defects during lay-up, which affect both local microstructure and geometry, their influence on tensile properties is surprisingly small in all cases when the sample was polymerized with a caul plate.

In order to complete this study it is important to quantify the influence of these singularities under other loading conditions. Tests have been performed under in-plane shear and compression loading, and results from these will be presented subsequently. The next step is to examine how these defects affect properties of more complex structures.

#### ACKNOWLEDGEMENTS

The authors would like to thank the region of Brittany (France) and the Regional Council of Morbihan for their financial support. The authors are also pleased to express their grateful acknowledgements to Mathieu Gestalin and Amaury Ducloux (Coriolis Composite) for the manufacture of plates by Automated Fibre Placement, and to Luc Riou (Ifremer) for the ultrasonic C-Scan analysis.

## REFERENCES

- [1] Lukaszewicz DH-JA, Ward C, Potter KD. The engineering aspects of automated prepreg layup: History, present and future. *Composites Part B: Engineering* 2012;43:997–1009. doi:10.1016/j.compositesb.2011.12.003.
- [2] Goldworthy WB. Geodesic path length compensator for composite-tape placement head. 3810.805, n.d.
- [3] Lukaszewicz DH-JA. Optimisation of high-speed automated layup of thermoset carbon-fibre preimpregnates. Ph.D. University of Bristol, 2011.
- [4] Lukaszewicz DH-JA, Potter KD. The internal structure and conformation of prepreg with respect to reliable automated processing. *Composites Part A: Applied Science and Manufacturing* 2011;42:283–92. doi:10.1016/j.compositesa.2010.11.014.
- [5] Lukaszewicz DH-JA, Potter KD, Eales J. A concept for the in situ consolidation of thermoset matrix prepreg during automated lay-up. *Composites Part B: Engineering* 2013;45:538–43. doi:10.1016/j.compositesb.2012.09.008.
- [6] Lopes CS, Gürdal Z, Camanho PP. Variable-stiffness composite panels: Buckling and first-ply failure improvements over straight-fibre laminates. *Computers & Structures* 2008;86:897–907. doi:10.1016/j.compstruc.2007.04.016.
- [7] Gürdal Z, Tatting BF, Wu CK. Variable stiffness composite panels: Effects of stiffness variation on the in-plane and buckling response. *Composites Part A: Applied Science and Manufacturing* 2008;39:911–22. doi:10.1016/j.compositesa.2007.11.015.
- [8] Cairns DS, Ilcewicz LB, Walker T. Far-field and near-field strain response of Automated Tow-Placed laminates to stress concentrations. *Composites Engineering* 1993;3:1087–97. doi:10.1016/0961-9526(93)90023-D.
- [9] Lopes CS, Gürdal Z, Camanho PP. Tailoring for strength of composite steered-fibre panels with cutouts. *Composites Part A: Applied Science and Manufacturing* 2010;41:1760–7. doi:10.1016/j.compositesa.2010.08.011.
- [10] Cairns DS, Ilcewicz LB, Walker T, Minguet PJ. Fracture scaling parameters of inhomogeneous microstructure in composite structures. *Composites Science and Technology* 1995;53:223–31. doi:10.1016/0266-3538(95)00022-4.
- [11] Blom AW, Stickler PB, Gürdal Z. Optimization of a composite cylinder under bending by tailoring stiffness properties in circumferential direction. *Composites Part B: Engineering* 2010;41:157–65. doi:10.1016/j.compositesb.2009.10.004.
- [12] Arian Nik M, Fayazbakhsh K, Pasini D, Lessard L. Surrogate-based multi-objective optimization of a composite laminate with curvilinear fibers. *Composite Structures* 2012;94:2306–13. doi:10.1016/j.compstruct.2012.03.021.
- [13] Arian Nik M, Fayazbakhsh K, Pasini D, Lessard L. A comparative study of metamodeling methods for the design optimization of variable stiffness composites. *Composite Structures* 2014;107:494–501. doi:10.1016/j.compstruct.2013.08.023.
- [14] Sawicki A, Minguet P. The effect of intraply overlaps and gaps upon the compression strength of composite laminates. 39th AIAA/ASME/ASCE/AHS/ASC Structures, Structural Dynamics, and Materials Conference and Exhibit, American Institute of Aeronautics and Astronautics; 1998.
- [15] Blom AW, Lopes CS, Kromwijk PJ, Gürdal Z, Camanho PP. A Theoretical Model to Study the Influence of Tow-drop Areas on the Stiffness and Strength of Variable-stiffness Laminates. *Journal of Composite Materials* 2009;43:403–25. doi:10.1177/0021998308097675.
- [16] Turoski LE. Effects of manufacturing defects on the strength of toughened carbon/epoxy prepreg composites /. 2000.

- [17] Croft K, Lessard L, Pasini D, Hojjati M, Chen J, Yousefpour A. Experimental study of the effect of automated fiber placement induced defects on performance of composite laminates. *Composites Part A: Applied Science and Manufacturing* 2011;42:484–91. doi:10.1016/j.compositesa.2011.01.007.
- [18] Legay P. Étude de l'influence de défauts sur les propriétés mécaniques de matériaux composites fabriqués par le procédé de placement de fibres. masters. École Polytechnique de Montréal, 2011.
- [19] Falcó O, Mayugo JA, Lopes CS, Gascons N, Costa J. Variable-stiffness composite panels: Defect tolerance under in-plane tensile loading. *Composites Part A: Applied Science and Manufacturing* 2014;63:21–31. doi:10.1016/j.compositesa.2014.03.022.
- [20] Rhead AT, Dodwell TJ, Butler R. The effect of tow gaps on compression after impact strength of robotically laminated structures. *Computers, Materials and Continua* 2013;35:1–16.
- [21] Falcó O, Lopes CS, Mayugo JA, Gascons N, Renart J. Effect of tow-drop gaps on the damage resistance and tolerance of Variable-Stiffness Panels. *Composite Structures* 2014;116:94–103. doi:10.1016/j.compstruct.2014.05.005.
- [22] Li X, Hallett SR, Wisnom MR. Modelling the effect of gaps and overlaps in automated fibre placement (AFP)-manufactured laminates. *Science and Engineering of Composite Materials* 2015;22:115–29.
- [23] Fayazbakhsh K, Arian Nik M, Pasini D, Lessard L. Defect layer method to capture effect of gaps and overlaps in variable stiffness laminates made by Automated Fiber Placement. *Composite Structures* 2013;97:245–51. doi:10.1016/j.compstruct.2012.10.031.
- [24] Arian Nik M, Fayazbakhsh K, Pasini D, Lessard L. Optimization of variable stiffness composites with embedded defects induced by Automated Fiber Placement. *Composite Structures* 2014;107:160–6. doi:10.1016/j.compstruct.2013.07.059.
- [25] Arian Nik M, Lessard L, Pasini D. Size-dependent behavior of laminates with curvilinear fibers made by automated fiber placement : *Science and Engineering of Composite Materials*. *Science and Engineering of Composite Materials* 2014;Volume 22:157–63.
- [26] <http://www.hexcel.com/fr/> 2015.
- [27] <http://www.coriolis-composites.com/> 2015.
- [28] American Society for Testing and Materials, ASTM D3039/ASTM D3039M, Test Method for Tensile Properties of Polymer Matrix Composite Materials. ASTM International; 2014.

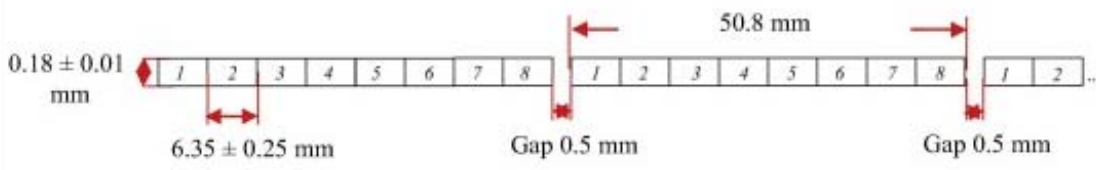


Fig. 1. Draping rule often imposed by aircraft manufacturers for the use of a tape laying head of  $n = 8$  ribbons

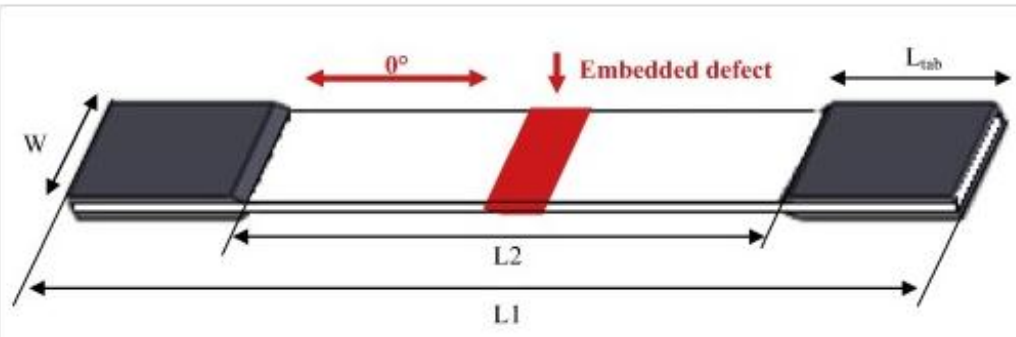


Fig. 2. Specimen geometry for tensile tests:  $L_1 = 250$  mm;  $L_2 = 150$  mm;  $L_{tab} = 50$  mm;  $W = 25$  mm

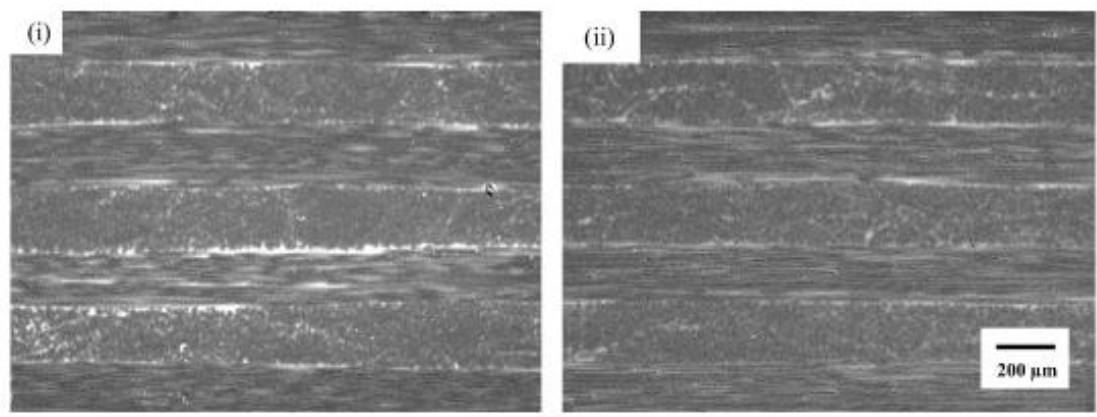
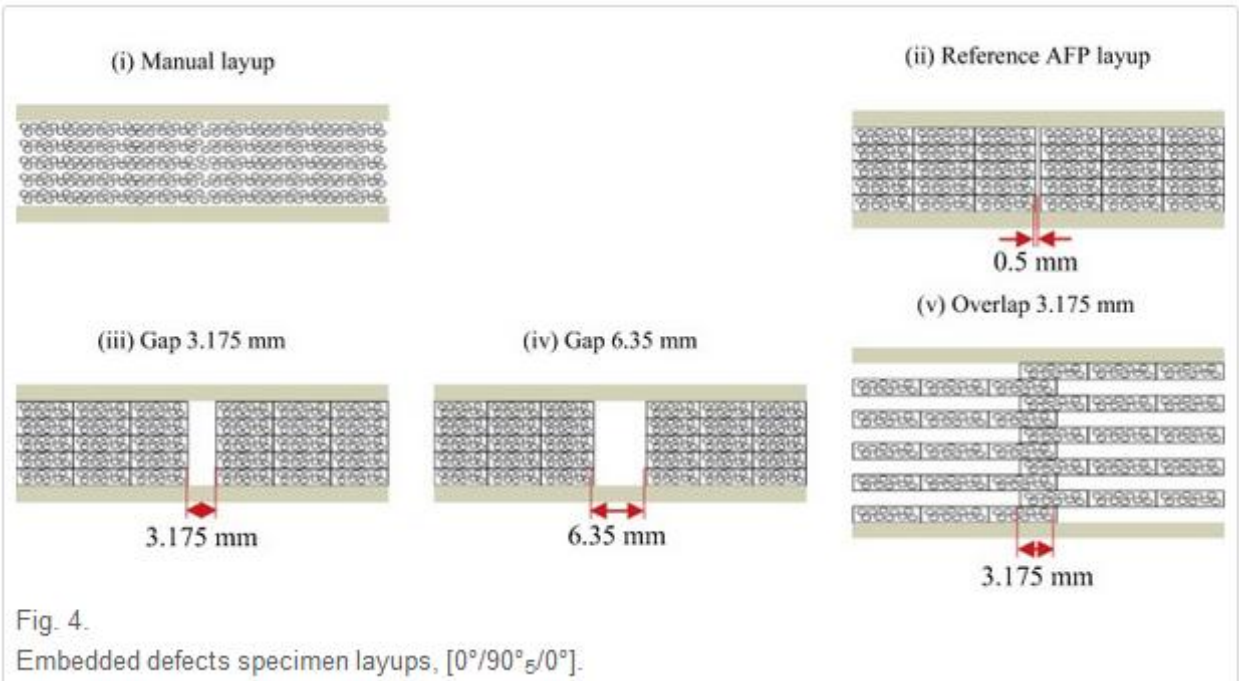


Fig. 3. Laminate microstructure of plates: (i) Manual layup; (ii) Automated layup



(i) - Manual layup, Without gaps, With caul plate



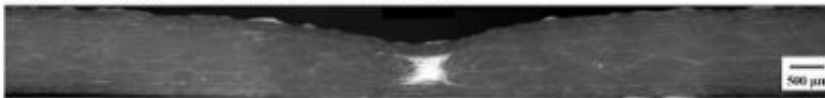
(ii) - AFP layup, Gap 0.5 mm, Without caul plate



(ii) - AFP layup, Gap 0.5 mm, With caul plate



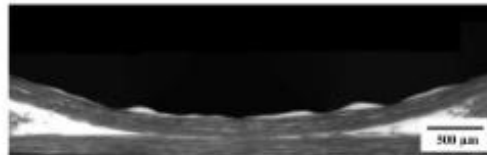
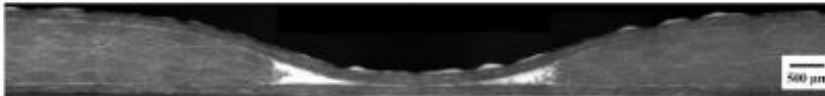
(iii) - AFP layup, Gap 3.175 mm, Without caul plate



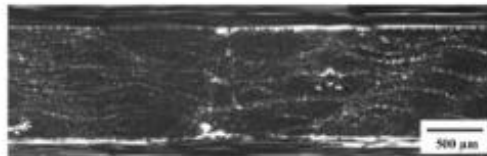
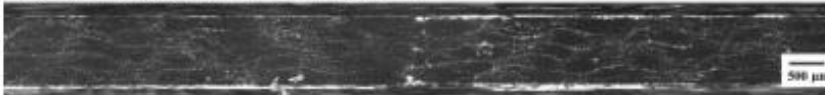
(iii) - AFP layup, Gap 3.175 mm, With caul plate



(iv) - AFP layup, Gap 6.35 mm, Without caul plate



(iv) - AFP layup, Gap 6.35 mm, With caul plate



(v) - AFP layup, Overlap 3.175 mm, Without caul plate



(v) - AFP layup, Overlap 3.175 mm, With caul plate



Fig. 5.

Microstructural SEM observations in the embedded defect region,  $[0^\circ/90^\circ_\pm/0^\circ]$ : (i) Manual layup; (ii) Reference AFP layup; (iii) AFP plate with a gap of 3.175 mm; (iv) AFP plate with a gap of 6.35 mm; (v) AFP plate with an overlap of 3.175 mm

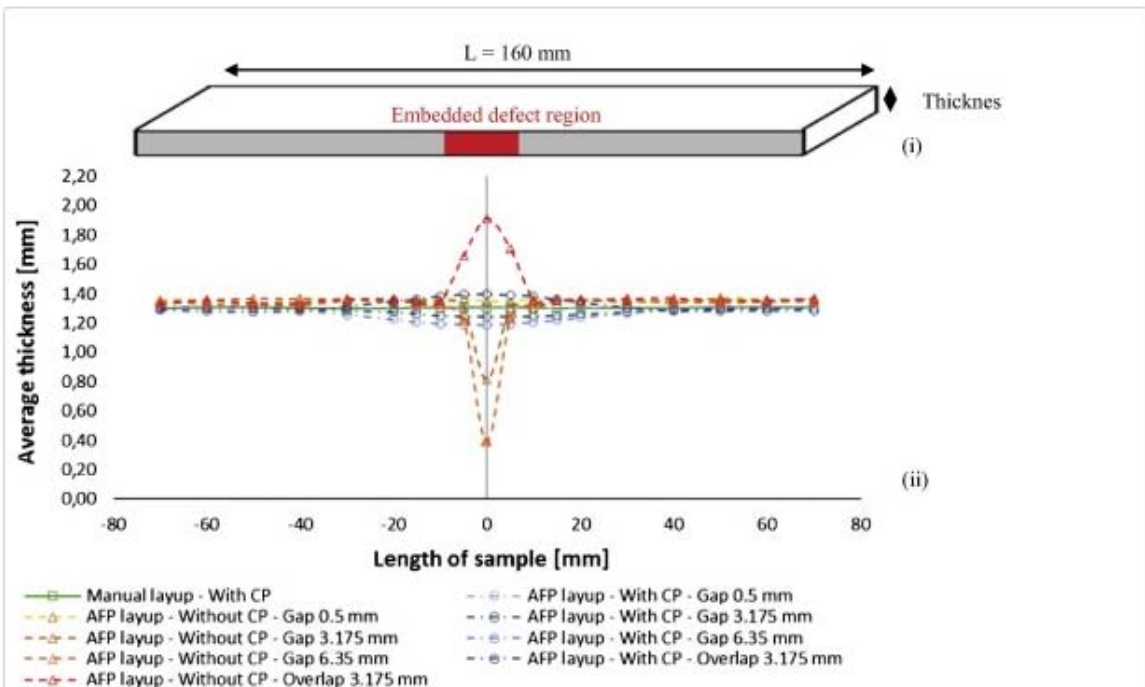


Fig. 6. (i) Specimen geometry for microstructure observations; (ii) Evolution of the thickness in the length of samples according to the embedded defects introduced during the draping phase,  $[0^\circ/90^\circ_\epsilon/0^\circ]$ . (For interpretation of the references to color in this figure legend, the reader is referred to the web version of this article.)

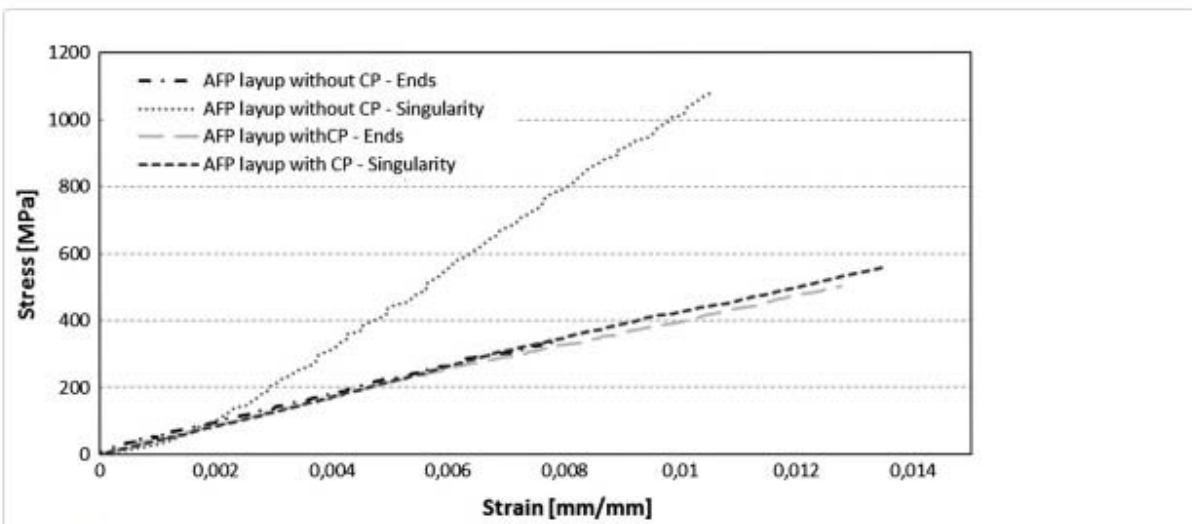


Fig. 7. Comparison of Stress-Strain for different gap 6.35 mm configuration (in the ends and embedded defect region of samples)

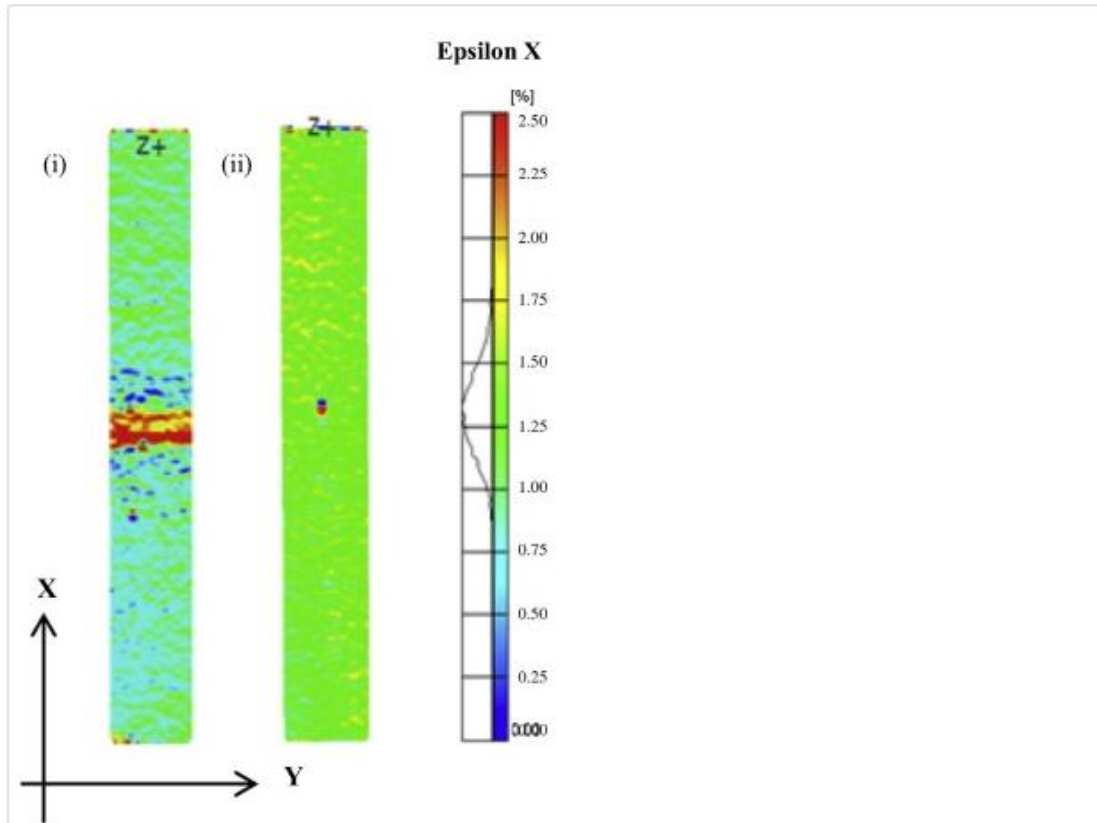


Fig. 8. Evolution of the axial deformation before rupture sample for gap 6.35 mm (ARAMIS): (i) Polymerized without caul plate; (ii) Polymerized with caul plate. (For interpretation of the references to color in this figure legend, the reader is referred to the web version of this article.)

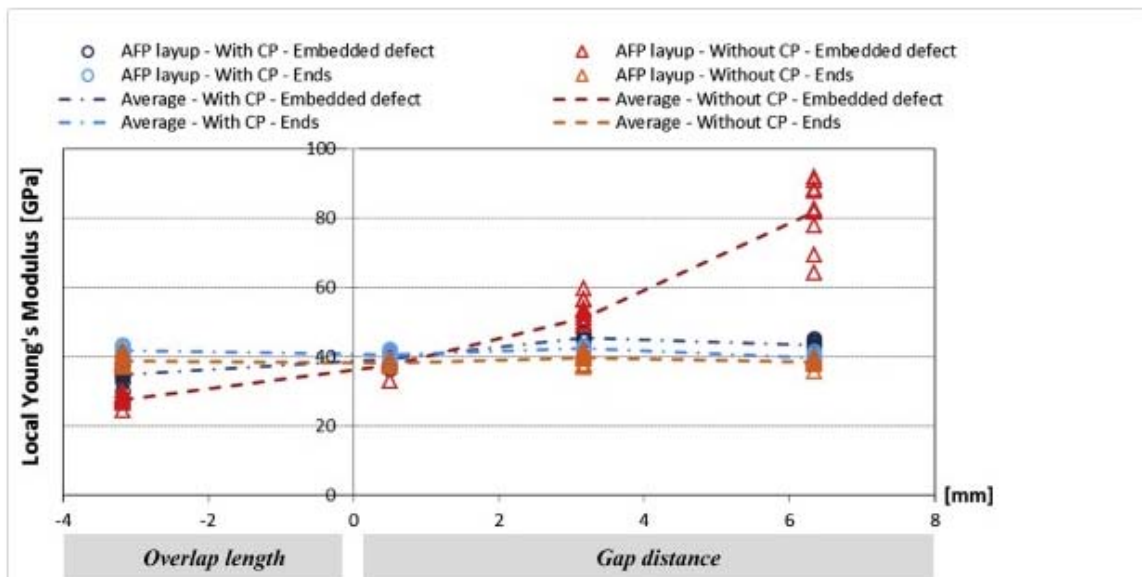


Fig. 9. Local elastic modulus variation (in the ends and embedded defect region of samples) as a function of the type of embedded defect with and without caul plate,  $[0^\circ/90^\circ_\pm/0^\circ]$ . (For interpretation of the references to color in this figure legend, the reader is referred to the web version of this article.)

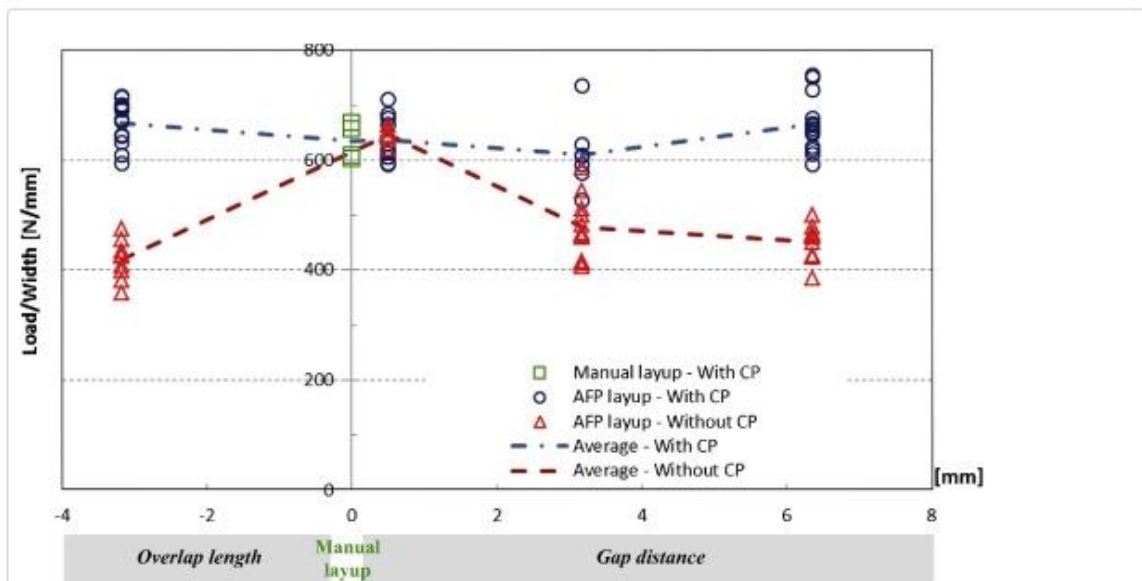


Fig. 10. Flow stress variation as a function of the type of embedded defect with and without caul plate,  $[0^\circ/90^\circ_\epsilon/0^\circ]$ . (For interpretation of the references to color in this figure legend, the reader is referred to the web version of this article.)

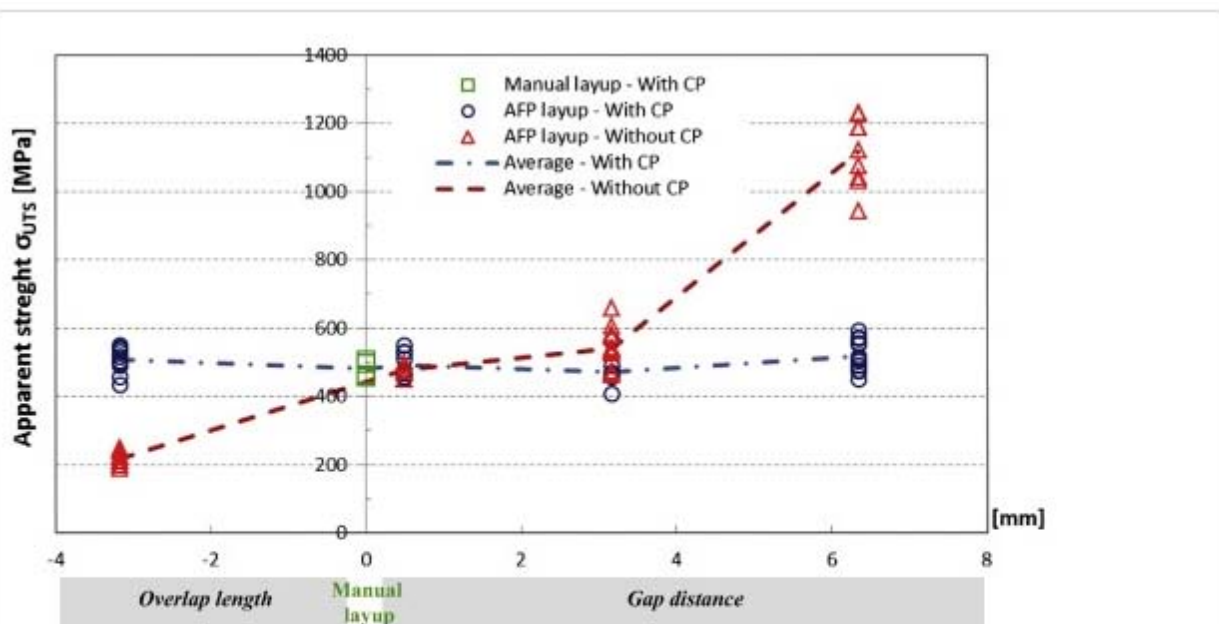
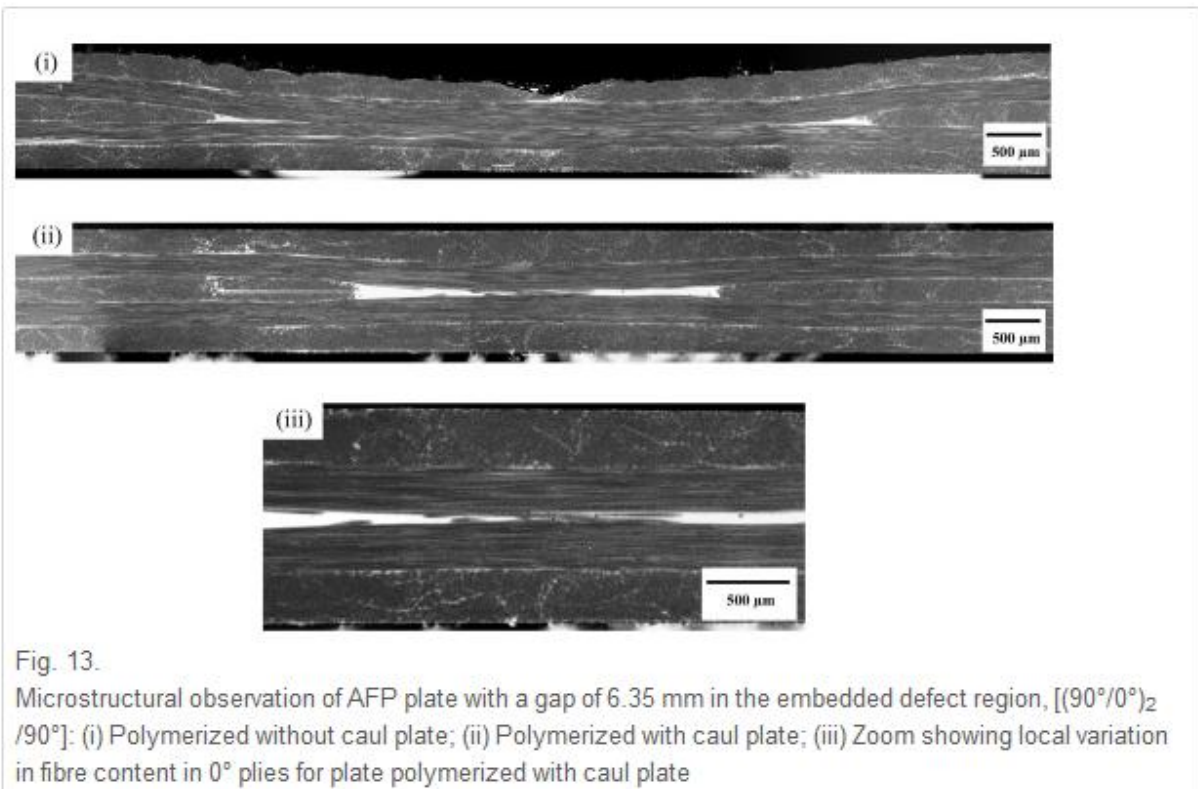
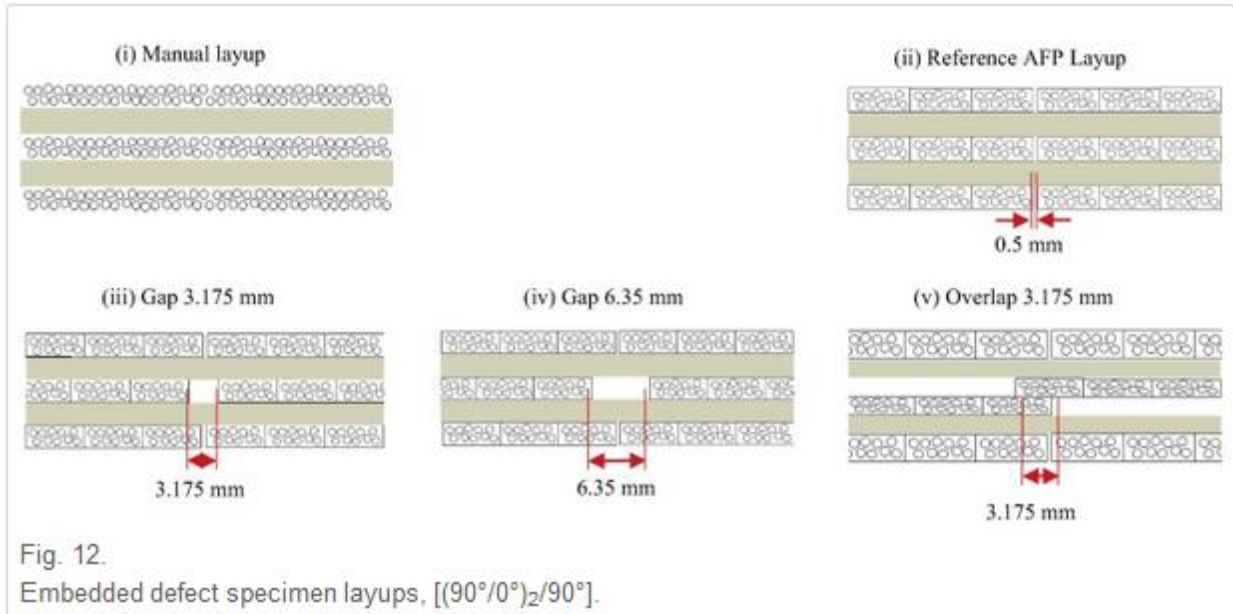
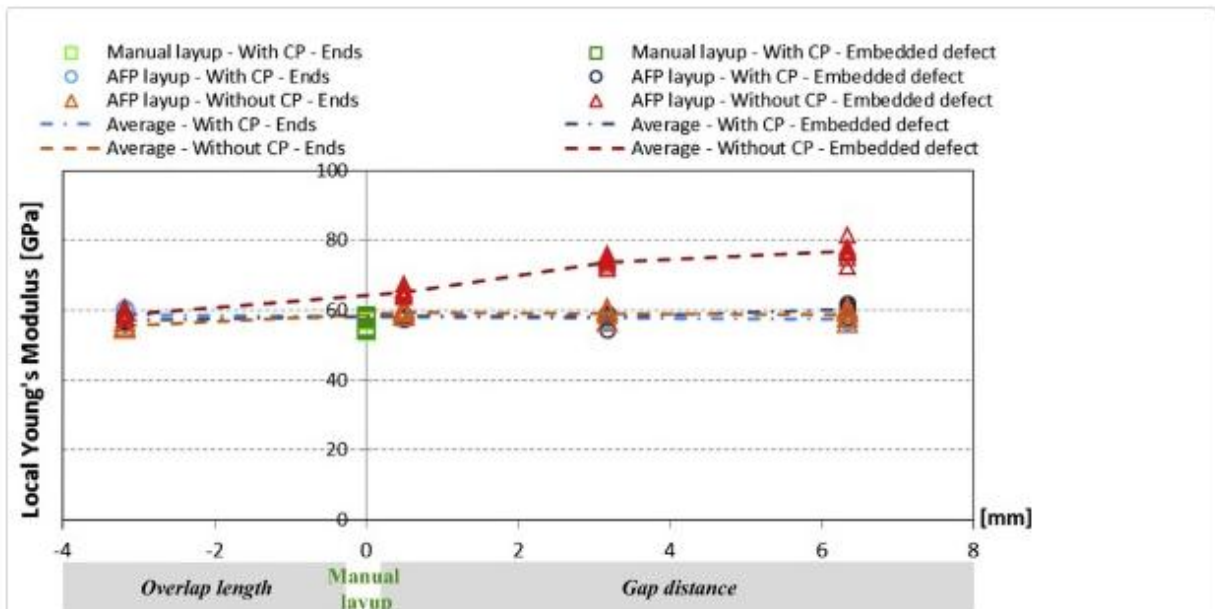
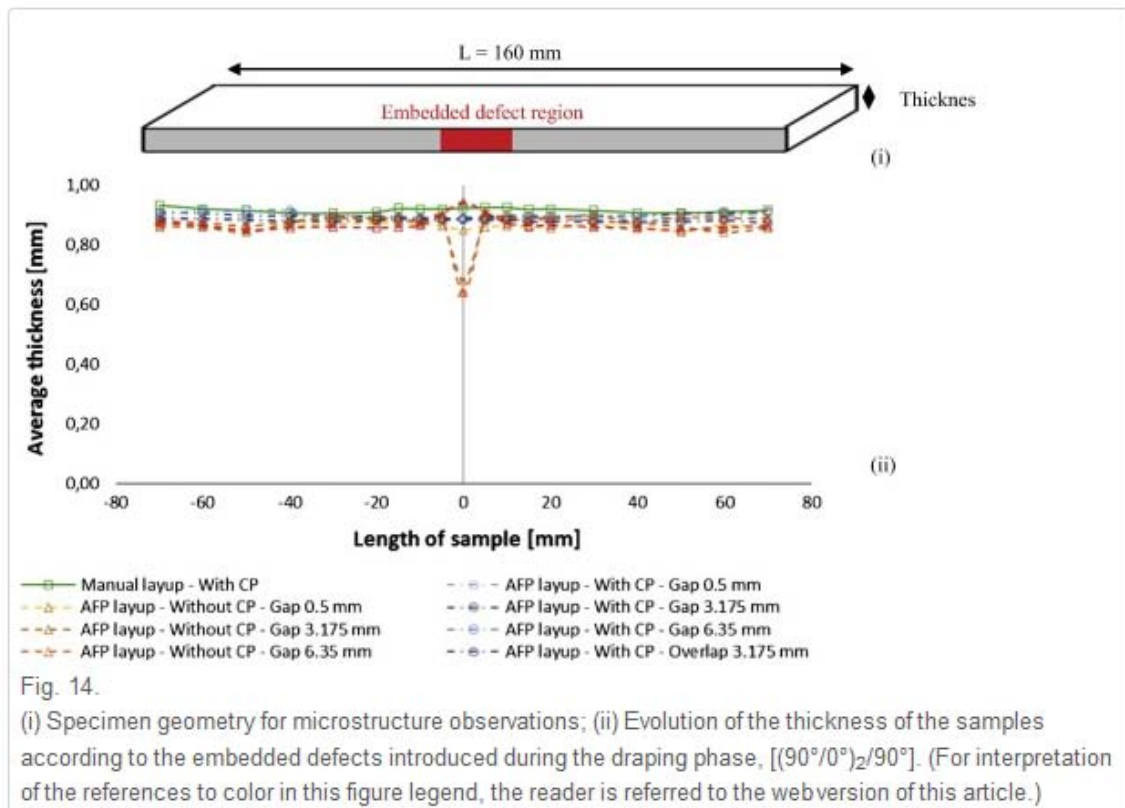


Fig. 11. Apparent tensile stress variation at failure as a function of the type of embedded defect with and without caul plate,  $[0^\circ/90^\circ_\epsilon/0^\circ]$ . (For interpretation of the references to color in this figure legend, the reader is referred to the web version of this article.)





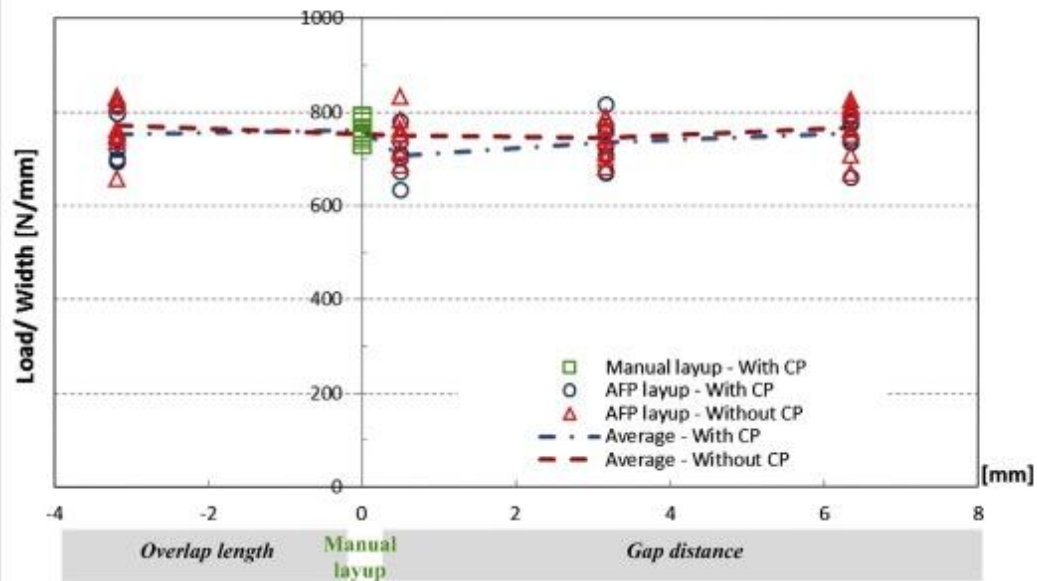


Fig. 16.

Flow stress variation as a function of the type of embedded defect with and without caul plate,  $[(90^\circ/0^\circ)_2/90^\circ]$ . (For interpretation of the references to color in this figure legend, the reader is referred to the web version of this article.)

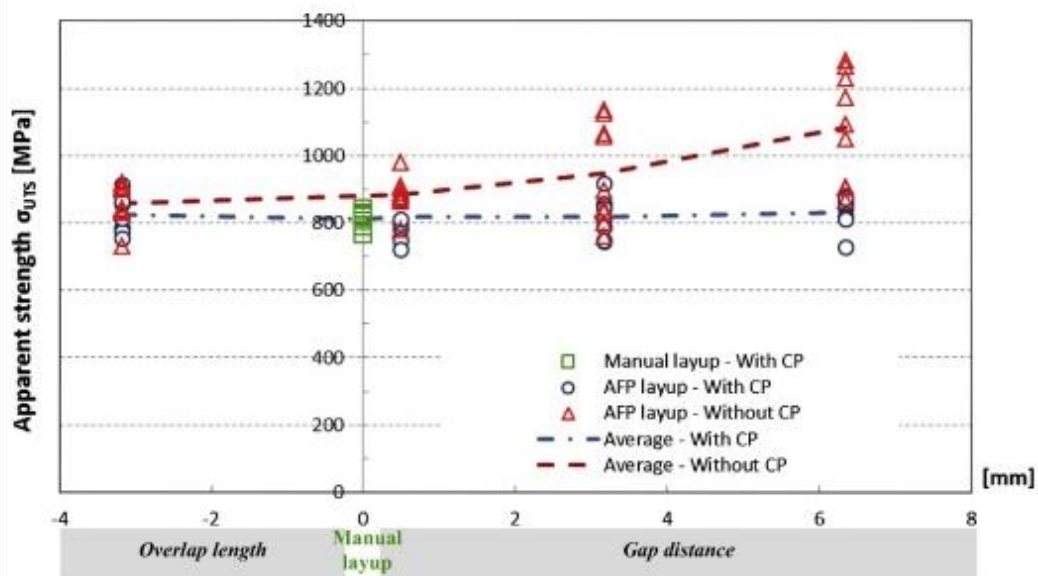


Fig. 17.

Apparent tensile stress variation as a function of the type of embedded defect with and without caul plate,  $[(90^\circ/0^\circ)_2/90^\circ]$ . (For interpretation of the references to color in this figure legend, the reader is referred to the web version of this article.)